

GASIFICATION AND COMBUSTION OF THE FOOTWEAR LEATHER WASTES

by

M. GODINHO, N. R. MARCILIO*, A.C. FARIA VILELA¹, L. MASOTTI, C. B. MARTINS

Departamento de Engenharia Química, Laboratório de Processamento de Resíduos

¹Programa de Pós-Graduação em Engenharia de Minas, Metalurgia e Materiais (PPGEM)
Universidade Federal do Rio Grande do Sul

RUA LUIZ ENGLERT S/Nº, ZIP CODE 90.040-040, PORTO ALEGRE-RS-BRAZIL

PHONE:+(55)(51)33083956; FAX:+(55)(51)30863277

ABSTRACT

One of the great technological challenges of this century is to identify alternative energy sources. The utilization of leather wastes (biomass) to generate energy becomes interesting due to its heating value, as well as for the characteristics of the ash generated, which could be used in other processes such as the production of basic chromium sulfate. Resulting from a partnership between research agencies and private businesses, a semi-pilot unit (350 kW_{th}) was designed and built to process leather wastes. The operation of this semi-pilot unit started in August, 2003. During this period, approximately 200 tons of wastes were treated in over 2,500 h of processing. The semi-pilot unit consists basically of a stratified downdraft gasifier, an oxidation reactor and an air pollution control system (APC). In this paper, the gasifier's emissions were evaluated and the ash and the flue gas were characterized.

ABSTRACTO

Uno de los grandes desafíos tecnológicos de este siglo es identificar fuentes de energía alternativa. La utilización de los residuos de cuero (biomasa) para generar energía se convierte interesante debido a su valor calórico, así como por las características de la ceniza generada, que se podría utilizar en otros procesos tales como la producción del sulfato básico del cromo. Resultante de una sociedad entre las agencias de la investigación y los empresas privadas, una unidad semi-piloto (kW_{th} 350) fue diseñada y construida para procesar residuos de cuero. La operación de esta unidad semi-piloto comenzó en agosto de 2003. Durante este período, aproximadamente 200 toneladas de residuos fueron tratados en más de 2.500 horas de proceso. La unidad semi-piloto consiste básicamente en un generador de gas estratificado de corriente descendente, un reactor de oxidación y un sistema de control de la contaminación atmosférica (APC). En este trabajo, las emisiones del generador de gas fueron evaluadas y la ceniza y el humo fueron caracterizados.

INTRODUCTION

The leather wastes generated by the footwear industry are considered dangerous due to the presence of trivalent chromium, derived from the salt utilized to tan hides. In Brazil, the majority of these wastes are disposed of in landfills and only about 3% are recycled.

In 2004, the Brazilian production of footwear for the domestic market was 755 million pairs, while 212 million pairs were produced for export.

The state of Rio Grande do Sul, located in Brazil's southern region, concentrates 40% of the country's footwear production, and is responsible for 75% of its footwear exports. The Brazilian footwear sector generated 166 thousand tons of wastes in 2004, of which nearly 50% are products that contain chromium. In 2003, Brazil was responsible for 5% of the world's footwear production and for 2.5% of its footwear exports.

Gasification is a thermal conversion process to produce, from fossil fuels, biomass and wastes, a combustible gas or a synthesis gas for subsequent utilization. In the process, several different types of gasification agents may be utilized, among these are air, O₂ and air/steam. There are currently approximately 160 gasification plants in operation in the world, and another 35 are being planned. Approximately 22% of the operating plants and 71% of those being planned are for the production of electricity¹. Aside from electricity, it is possible to produce in these plants hydrogen, ammonia, syngas and methanol, among other products.

Gasification is an attractive process for reducing the possibility of the formation of PCDD/F due to the reducing conditions². In downdraft gasifiers, the tar content in the combustible gas is reduced by a factor of nearly 100, because the pyrolysis products are partially oxidized in the hearth zone³.

Research on the gasification of several types of fuels has been conducted in recent years, mostly related to coal¹, wastes⁴, and biomass⁵. However, there are rarely no studies related to

footwear leather wastes gasification. Experiments for the gasification of wastes from tanneries (sludge, shavings, trimmings, hair, buffing dust, and others) were conducted in a downdraft gasifier. The gasifier has a capacity of 70 kg of dry wastes per hour. When the gasifier is operated at 50 kg per hour, approximately 120 Nm³ per hour of combustible gas is generated, with an approximate heating value of 5 MJ per Nm³. The characterization of the ash generated in the experiments conducted with chrome shavings indicated a concentration of 1.2 % (w/w) of Cr (VI)⁶.

The objective of this paper is to evaluate the performance of a semi-pilot unit for the processing of footwear leather wastes. The unit is basically composed of a stratified downdraft gasifier, an oxidation reactor and an air pollution control system (APC).

EXPERIMENTAL

Figure 1 shows a flowchart of the semi-pilot unit (350 kW_{th}), while Figure 2 presents a schematic representation of the stratified downdraft gasifier and the oxidation reactor.

The waste is fed into the gasifier through a ram feed system. The use of this system is due to the fact that in fixed bed gasifiers there is no need to shear the leather scrap before feeding. The downdraft is a co-current gasifier, in which the waste is fed from the top and the gasification agent is introduced at the sides above the grate, while the combustible gas is withdrawn from under the grate (reduction zone)⁷. The description of the zones present in a stratified downdraft gasifier can be found somewhere else⁸.

The gasifier is internally lined with refractory material (silica-alumina) and has a square cross-section with total volume of 0.66 m³. Two kerosene burners are used to start up the unit. The ash is removed by a screw conveyor located at the bottom of the gasifier.

The primary air is injected immediately below the grate (primary combustion zone-PCZ), where the reactions with the

	x (mean value)	s (standard deviation)
Moisture (% wt)	14.1	1.4
<i>Proximate analysis(%wt;d.b.)</i>		
Volatile matter	77.3	2.2
Ash	5.8	0.5
Carbon fixed*	16.9	1.2
<i>Ultimate analysis(%wt;d.b.)</i>		
S	1.83	0.25
C	49.31	0.80
H	8.52	0.08
N	12.42	0.49
Cl	0.45	0.14
Cr	2.77	0.32
O*	24.70	0.88
HHV(kcal/kg)	4406.3	241.6

* by difference, d.b.: dry basis

combustible gas begin. This zone (A=0.380 m² and V=0.160 m³) has the same configuration as the gasifier. In the secondary combustion zone-SCZ (A= 0.06 m² and V= 0.04 m³), an increase in the turbulence occurs with the objective of increasing combustion efficiency. The secondary air exchanges heat to cool the grate. Most of the air necessary for the complete oxidation of the combustible gas is injected in the tertiary combustion zone-TCZ (A= 0.742 m² and V= 0.460-m³). The final stage of the combustion occurs in the quaternary combustion zone-QCZ (A= 0.138 m² and V= 0.07 m³), located downstream of the tertiary combustion zone.

Downstream is the air pollution control system (APC), composed of a cyclone, an air-cooled heat exchanger, a venturi scrubber, a packed wet scrubber and a jet venturi scrubber. The cyclone is cooled by a jacketed wall (natural convection). The heat exchanger has a jacketed wall with longitudinal fins where it drains an air stream (forced convection). In the venturi

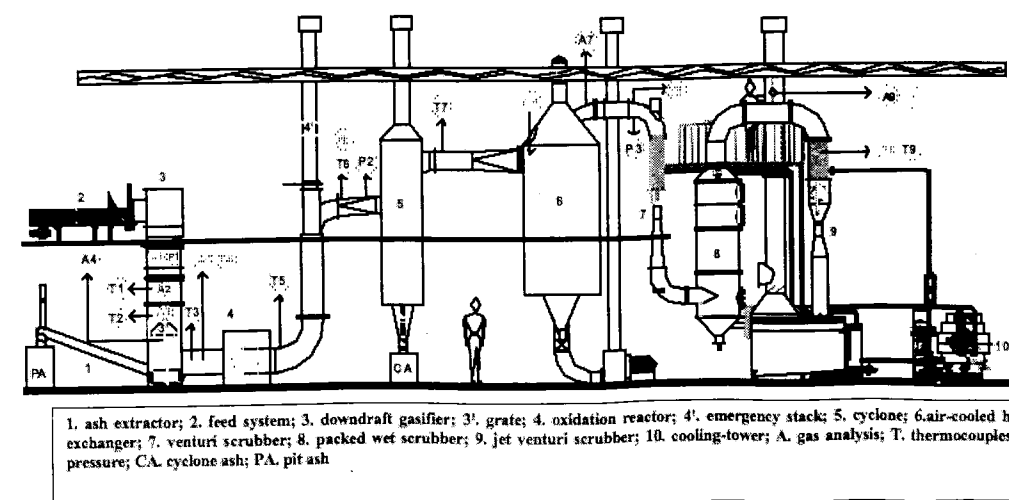


Figure 1: Semi-pilot unit

* Corresponding Author - E-mail: nilson@enq.ufrgs.br

Manuscript Received June 26, 2006, accepted for publication January 4, 2007

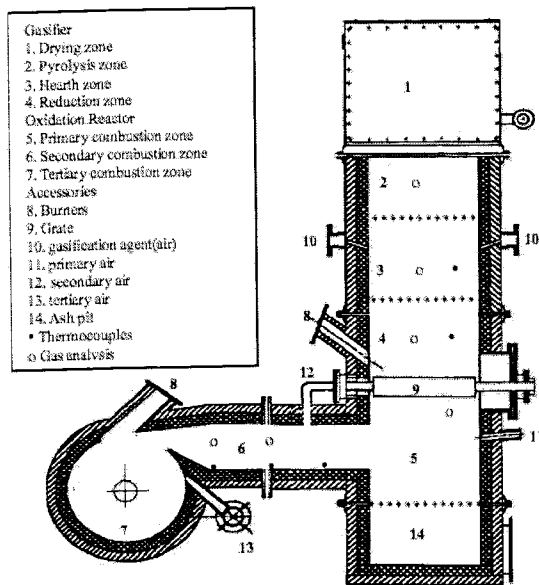


Figure 2. Downdraft gasifier and oxidation reactor

scrubber an alkaline solution is injected, which reacts with the acid gases (SO_2/HCl) formed in the process. The pressure drop across the unit is overcome by draft in the jet venturi scrubber.

The pressures and temperatures were continuously monitored during the analyses. The concentration of gases (O_2 , CO , CO_2 , NO , CH_4) was determined with the GreenLine 8000 analyzer, manufactured by Eurotron Instruments S.p.A. The concentration of O_2 , CO , NO was determined using electrochemical cells, while the concentration of the CO_2 and the CH_4 were measured by an infrared spectrometer (IR). Chlorides were determined by mercury nitrate, and sulfates by turbidimetry.

The US EPA Method 3060A was used to determine the Cr (VI) in the ash samples. The ash particle-size distribution was determined with a laser particle size analyzer from CILAS, which allows the measurement of particles between 0.04 and 2,500 μm .

The ash composition was determined by X-ray fluorescence (XRF) and X-ray diffraction (XRD). The XRF and XRD analyses were conducted in a Rigaku RIX 2000 and a Siemens D 5000, respectively.

The particulate matter characterization was conducted according to US EPA Method 17 at two points of the unit (A8 and A9). This method is based on isokinetic sampling of flue gas.

The determination of the concentration of hydrochloric acid and chlorine gas in the flue gas was conducted in accordance to US EPA Method 50.

Fuel Characterization

The characterization of the footwear leather wastes was done starting from a random collection of three samples, obtained from a footwear industry residue center. The samples used contain chromium (scrap leather), which represents nearly 50% of the total of residues received by the center. The results of the analysis are presented in Table I.

TABLE II
Composition of the Combustible Gas (d.b.)

	x	s
T2(°C)	506.7	47.3
Gas	mole fraction	
CO	0.061	0.003
CO ₂	0.132	0.016
CH ₄	0.118	0.008

TABLE III
Ash particle-size distribution

ϕ_p	PA	ϕ_p	CA
mean	403 ηm	mean	17 ηm
< 37 μm	15.3%	< 3.5 μm	10.0%
< 598 μm	49.9%	< 14.0 μm	50.0%
< 1,205 μm	71.7%	< 44.0 μm	90.0%

TABLE IV
Cr(VI) Concentration in the CA

m_{sample} [g]	Abs[540 nm]	Cr VI [ppm]
1.07	0.0043	0.82
2.00	0.1501	9.60
1.50	0.0403	3.60
1.50	0.0425	3.79
1.50	0.1001	8.62
2.04	0.1315	8.28
2.00	0.0731	4.76

The samples contain high quantities of volatile matter and low presence of inorganic material (ash), while their heating value enables combustion under auto-thermal conditions. Based on the results, it is possible to observe that the waste has a high nitrogen concentration, since animal skin is basically formed of protein and water. Nearly 95% of the protein present in the skin is collagen.

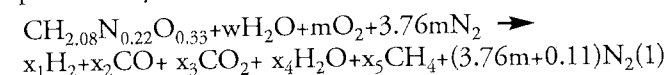
The presence of chromium is due to the tanning of the hides, which is done with salts of this element ($\text{Cr}(\text{OH})\text{SO}_4$). Most of the chlorine present is from an inorganic origin, since sodium chloride (NaCl) is utilized as preservative for the hides, and also added in the pickle. Several sulfur compounds are utilized in the hide tanning process. Among those are the sulfide, added in the depilation stage, the ammonium sulfate and the sodium hydrogen sulfite, applied during the delimiting, and the tanning agent itself.

RESULTS AND DISCUSSION

Energy and Mass Balance

The gasifier's energy and mass balance was done to estimate the composition of the combustible gas. The system was resolved according to methodology proposed elsewhere^{9,10}.

The gasification of the footwear leather waste can be represented by the reaction (1):



For the solution of the system, it is assumed that the reactions are in thermodynamic equilibrium and the gasification process is adiabatic. The chemical equilibrium is based on the reactions (2) and (3).



The system is composed of the equations below:
Equilibrium:

$$K_{\text{reaction}(2)} = \frac{x_5}{(x_1)^2} \quad (\Delta H = -75.0 \text{ kJ.mol}^{-1})$$

$$K_{\text{reaction}(3)} = \frac{x_3 x_1}{x_2 x_4} \quad (\Delta H = -41.2 \text{ kJ.mol}^{-1})$$

Mass balance

$$1 = x_2 + x_3 + x_5 \quad (\text{carbon})$$

$$2w + 2.08 = 2x_1 + 2x_4 + 4x_5 \quad (\text{hydrogen})$$

$$w + 0.33 + 2m = x_2 + 2x_3 + x_4 \quad (\text{oxygen})$$

Energy balance

$$H_{\text{fuel}}^0 + w(H_{\text{H}_2\text{O}(l)}^0 + H_{\text{H}_2\text{O}(g)}^0) + mH_{\text{O}_2}^0 + 3.76mH_{\text{N}_2}^0 = x_1H_{\text{H}_2}^0 + x_2H_{\text{CO}}^0 + x_3H_{\text{CO}_2}^0 + x_4H_{\text{H}_2\text{O}(v)}^0 + x_5H_{\text{CH}_4}^0 - (T_2 - T_1)(x_1C_{\text{P H}_2} + x_2C_{\text{P CO}} + x_3C_{\text{P CO}_2} + x_4C_{\text{P H}_2\text{O}(v)} + x_5C_{\text{P CH}_4} + (3.76m + 0.11)C_{\text{P N}_2})$$

A parameter commonly used in gasification processes is the equivalence ratio (ϕ), which may be defined as the O_2 fraction of the stoichiometric O_2 amount used to complete the combustion. Using the air as the gasification agent, the estimated composition of the combustible gas, as a function of the equivalence ratio, is represented in Figure 3.

The analyses to determine the emissions of the gasifier were conducted at point A4, presented in Figure 1. Throughout the analyses, the equivalence ratio remained approximately 0.4. The concentrations of the combustible gas are presented in Table II. The concentrations determined at the exit of the gasifier are consistent with the values estimated by the energy and mass balance.

The lower heating value of the combustible gas (LHV_{gas}) was estimated based on the equation (4), while the equation (5) was utilized to estimate the gasification efficiency (η_G). Figure 4 presents the results obtained from the balance of mass and energy of the gasification reactor, for the gasification efficiency and the lower heating value of the combustible gas.

$$\text{LHV}_{\text{gas}} \left(\frac{\text{MJ}}{\text{Nm}^3} \right) = \frac{y_{\text{H}_2}(\Delta H_o)_{\text{H}_2} + y_{\text{CO}}(\Delta H_o)_{\text{CO}} + y_{\text{CH}_4}(\Delta H_o)_{\text{CH}_4}}{22.4 \cdot 10^3} \quad (4)$$

TABLE V
Ash X-ray Fluorescence (%wt; d.b.)

	Pit Ash (PA)	Cyclone Ash (CA)
Cr ₂ O ₃	55.91	32.24
SiO ₂	23.58	19.86
Al ₂ O ₃	7.35	7.10
SO ₄	2.81	9.54
Fe ₂ O ₃	2.59	15.48
TiO ₂	1.53	2.26
P ₂ O ₅	1.59	4.09
CaO	1.20	2.51
Na ₂ O	1.08	2.90
K ₂ O	0.79	0.85
Cl	0.72	1.12
MnO	ND	0.05
MgO	ND	1.20

ND: not detectable

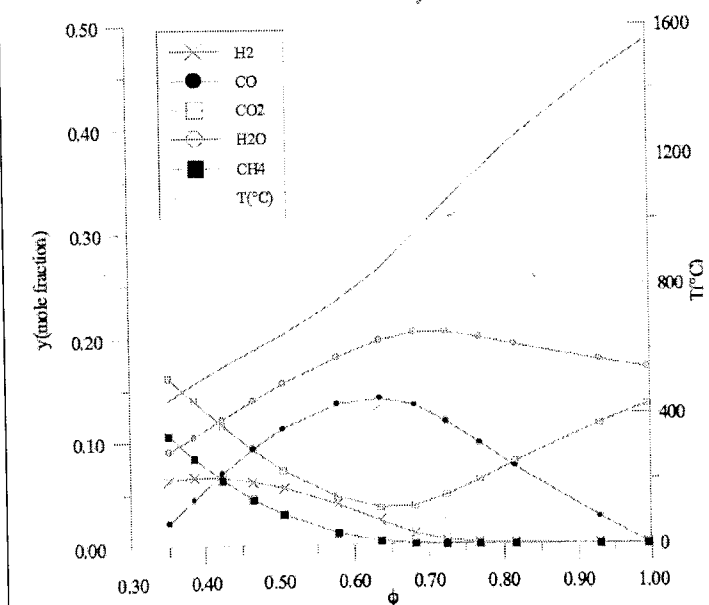


Figure 3 - Estimated composition of the combustible gas (data obtained at atmospheric pressure)

$$\eta_G = \frac{m' \text{LHV}_{\text{gas}}}{\text{HHV}_{\text{waste}} \cdot 4.19 \cdot 10^{-3}} \cdot 100 \quad (5)$$

The gasification reactor operates with an equivalence ratio of approximately 0.4, which represents gasification efficiency between 82 and 84%, with the generation of a combustible gas with lower heating value close to 4.0 MJ.Nm^{-3} .

Ash Characterization

The particles collected at the bottom of the gasifier (PA) have a diameter significantly larger than that of the ones collected in the cyclone (CA). The ash particle-size distribution is presented in Table III. The PA/CA ratio (w/w) is

TABLE VI
Particulate Matter Characterization (A8)

Fuel throughput	[kg/h]	max. 70	
Technical Data			
Gasifier temperature (T2)	[°C]	x	s
Oxidation reactor temperature (T4)	[°C]	557	21.2
Flue gas temperature (T9)	[°C]	914	25.4
Cyclone pressure (P2)	[mmH ₂ O]	32.3	2.2
Venturi scrubber flow rate	[m ³ /h]	40.5	2.1
Sodium hydroxide 50% (w/w)	[ml/min]	2.9	0.1
Flue gas moisture	[%v/v]	49	1.4
Flue gas velocity	[m/s]	4.8	0.2
Flue gas velocity	[m/s]	3.3	0.2
Particulate Matter Characterization (A8)			
Particulate matter concentration	[mg/Nm ³]	131.1	29.5
(sodium chloride/particulate matter) ratio	[%w/w]	4.43	0.06
(sodium sulfate/particulate matter) ratio	[%w/w]	31.54	14.4
(soluble material/particulate matter) ratio	[%w/w]	80.5	3.8
Mean particle diameter	[μm]	6.5	0.4

TABLE VII
Packed Wet Scrubber's Bottom Solution

Time (h)	Chloride (mg/L)		Sulfate (mg/L)		Solid suspension (mg/L)		Cl/SS	SO ₄ /SS
	x	s	x	s	x	s		
0	525	151	719	44	55	27		
4	7,823	1,893	18,604	457	1,224	116	6.4	15.2
8	16,670	3,342	26,570	4,397	1,681	511	9.9	15.8

TABLE VIII
Particulate Matter Characterization (A9)

Fuel throughput	[kg/h]	max. 70	
Technical Data			
Gasifier temperature (T2)	[°C]	x	s
Oxidation reactor temperature (T4)	[°C]	526	18.4
Flue gas temperature (T10)	[°C]	905	20.1
Cyclone pressure (P2)	[mmH ₂ O]	31.3	1.4
Venturi scrubber flow rate	[m ³ /h]	47.9	5.3
Sodium hydroxide 50% (w/w)	[ml/min]	2.9	0.1
Jet venturi scrubber flow rate	[m ³ /h]	6.0	0.1
Flue gas moisture	[%v/v]	3.8	0.1
Flue gas velocity	[m/s]	1.1	0.1
Flue gas flow rate	[m ³ /h]	464.3	1.2
Flue gas flow rate	[Nm ³ /h]	396.7	0.6
Particulate Matter Characterization (A9)			
Particulate matter concentration	[mg/Nm ³]	55.0	20.7
(soluble material/particulate matter) ratio	[%w/w]	48.2	5.8

TABLE IX
Hydrochloric Acid and Chlorine Gas Concentration

	F _{vs} (m ³ /h)	R	F _R (kg/h)	F _{jvs} (m ³ /h)	R	F _R (kg/h)	HCl*		Cl ₂ *	
							x	s	x	s
A9	2.8	NaOH**	2.3	6.0	None	None	24.55	3.04	26.87	4.45
A9	2.8	NaOH**	2.7	6.0	CaO	1.60	ND	ND	37.33	2.49
A9	2.8	NaOH**	2.7	7.2	NaOH**	1.45	ND	ND	ND	ND

ND: not detectable

*7%O₂; dry basis

**NaOH 50%(w/w)

TABLE X
Operational Parameters of the Combustion Zones*

Zone	T(°C)	F _{air} (Nm ³ /h)	F _{air} (m ³ /h)	v(m/s)	Re	τ _{ideal} (s)
PCZ	800-850	45-65	784	0.6	2,284	0.74
SCZ	900-960	65-85	1,167	5.6	8,358	0.13
TCZ	780-840	125-145	1,586	0.6	3,850	1.04
QCZ	700-750	0	1,462	2.9	9,550	0.17

*F_{gasification agent}: 130-150 Nm³/h; Fuel throughput: max 70 kg/h

approximately 30, which means that for every 30 kg of ash deposited in the ashtray, 1 kg is collected in the cyclone.

Both ashes have a carbon concentration lower than 0.5% (w/w), suggesting a good performance of the combustion¹¹.

The concentration of Cr(VI) in the CA was less than 10 ppm in all samples, as shown in Table IV. The low concentration of Cr(VI) may be attributed to the reducing conditions applied during the gasification of the waste, and to the fuel-rich environment in the primary and secondary combustion zones.

The X-ray fluorescence (Table V) indicated that the main elements present in the PA were chromium, silicon and aluminum. The components present in the ash from leather scrap incineration have Al₂O₃ concentration between 0.1% and 6%, and SiO₂ concentration between 0.07 and 22.2%¹².

The X-ray diffraction identified the presence of eskolite (Cr₂O₃), quartz (SiO₂), cristobalite (SiO₂) and aluminum chromite (Fe(Al,Cr)₂O₄) in both ashes.

Flue Gas Characterization

Particulate Matter

The mean value (x) presented in Table VI refers to the analyses conducted at point A8. In this Table, the operational parameters of the unit and the particulate matter characterization are presented.

Based on the results, it was possible to determine that a large portion of the material retained in the filters were water-soluble particles. Both the sodium chloride and the sodium sulfate

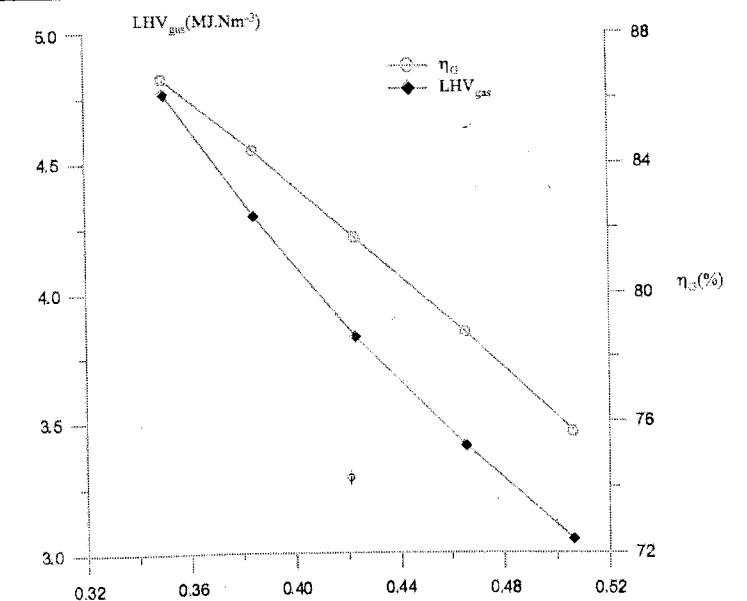


Figure 4: Gasification efficiency and lower heating value of the combustible gas

are formed in the reaction of the sodium hydroxide with the hydrochloric acid and the sulfur dioxide, respectively. However, the total mass of the soluble material present in the filters is larger than the mass of these compounds. This difference occurs possibly due to the reaction of the sodium hydroxide with the carbon dioxide, forming sodium carbonate, and to the dragging of sodium hydroxide by the flue gas.

The increase in the concentration of sulfate (SO₄²⁻) and

TABLE XI
NO Concentration

		x	s
NO*	[mg/Nm ³]	445.8	86.5
T2	[°C]	582.9	90.5
T4	[°C]	938.4	74.3

*11%O₂;d.b.

chloride (Cl⁻) in relation to the increment in the concentration of solid suspension in the packed wet scrubber's bottom solution, may be seen in Table VII. The relation between the sulfate and the solid suspension (SO₄/SS) was around 15, while the relation between the chloride and the solid suspension (Cl/SS) suffered significant variation, possibly due to the higher standard deviation observed in the chlorine's ultimate analysis.

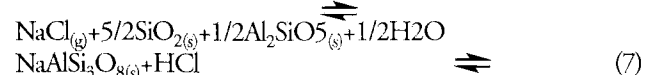
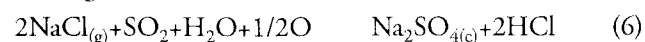
The particulate matter characterization for point A9 of the unit is presented in Table VIII.

The dilution of soluble solids in the jet venturi scrubber caused a reduction in the particulate matter concentration in the analysis conducted for point A9.

HCl/Cl₂ emissions

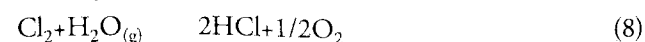
Experiments were conducted under several operating conditions of the APC to evaluate the concentration of hydrochloric acid (HCl) and chlorine gas (Cl₂) in the flue gas. The results are presented in Table IX.

The sodium chloride is the main source of chlorine in leathers. The behavior of NaCl at high temperatures and the relationships between Cl₂, HCl, NaCl(g) and NaCl(c) were studied elsewhere¹³. The partial pressure of equilibrium for NaCl at 967°C is 3,130 ppm. The NaCl(g) may be converted into HCl according to the reactions (6) and (7).



The increase in the concentration of sulfate ions (SO₄) in the CA and the availability of oxygen and sulfur dioxide suggest that the reaction (6) is occurring in the oxidation reactor.

The Cl₂ is formed by oxidation of HCl according to the Deacon reaction (8). The formation of Cl₂ is thermodynamically favored by temperatures lower than 800 K¹⁴.



The Cl₂ has limited solubility in water (0.0057gCl₂/gH₂O; 30°C), forming a mixture of hypochlorous and hydrochloric acids, according to the reaction (9):



The Cl₂ reacts with a solution of sodium hydroxide to form a mixture of sodium chloride and sodium hypochlorite, according to the reaction (10).

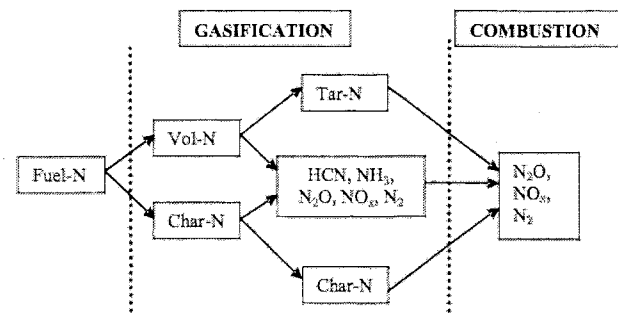
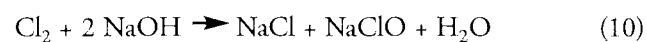


Figure 4: Fuel-bound nitrogen mechanism



The addition of lime (CaO) in the jet venturi scrubber increased the efficiency of the HCl removal, but presented low efficacy for the Cl₂, while the use of sodium hydroxide in the jet venturi scrubber eliminated the emission of both compounds.

CO emissions

The main variables that determine the combustion efficiency of a process are: residence time, turbulence, and the temperature. The residence time in combustion processes depends largely on the air flow introduced in the combustion chamber¹⁵. The ideal residence time (τ) may be estimated with equation (11):

$$\tau_{ideal} = \frac{0.098.V.P}{m_{air}.T} \quad (11)$$

The degree of mixture (turbulence) between the reactants is determined by the Reynolds number (Re), and may be defined by equation (12). The transition from laminar to turbulent flame occurs at Reynolds number in the range of 2,000 to 10,000. For carbon monoxide and city gas, the flame becomes turbulent in the range of 4,800 to 5,000 and 6,400 to 9,200, respectively¹⁶.

$$\text{Re} = \frac{\rho.v.L}{\mu} \quad (12)$$

The maximum temperature of the flue gas may be estimated by the global balance of energy (oxidation and gasification reactors), represented by equation (13).

$$\sum x_{in} [H_f^o + \Delta h] - \sum x_{out} [H_f^o + \Delta h] \quad (13)$$

For excess oxygen of 9% and 11% (v/v), on a dry basis, the maximum temperature obtained was 1,042°C and 909°C, respectively. Table X presents operational parameters (average value) of the combustion zones of the unit.

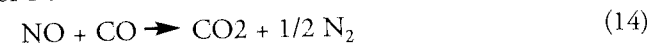
With the oxidation reactor operating according to the parameters presented on Table X, the CO emissions remained below 20 ppm.

NO_x emissions

Due to the absence of high temperature regions (T>1,500°C) in the unit, the main mechanism for the formation of nitrogen oxides (NO_x) is the fuel-bound nitrogen, schematically presented in Figure 4. In the pyrolysis zone, part of the fuel-N is released into the gas-phase (Vol-N) and part is retained in the char (Char-N)¹⁷.

The main precursors of nitrogen oxides are the HCN and NH₃. It is not clear whether the HCN and the NH₃ are released independently, or the NH₃ is a product of the HCN hydrolysis¹⁸.

Studies were conducted to evaluate the reaction of the NO with the CO (reaction 14) in the presence of quartz. It was observed that the most important variable for the NO reduction is the CO concentration. NO conversions close to 0.7 were obtained with an initial NO concentration of 1,000 ppmv, temperature of 1,073 K, CO concentration of 3% (v/v) and residence time of 1 s¹⁹.



Experiments were conducted in 0.1 MW_{th} bubbling fluidized bed pilot plant utilizing footwear leather wastes²⁰. The NO emissions were between 1,360 mg.Nm⁻³, at 900°C, and 1,400 mg.Nm⁻³, at 800°C (11% O₂). The NO concentration measured at point A7 of the unit is presented in Table XI.

The presence of quartz and CO in the combustible gas oxidation region indicates that the NO reduction, in relation to the values found in fluidized bed, is due to reaction (14).

CONCLUSIONS

From the results obtained in this study, it is possible to conclude that:

The operational conditions applied in the process provided a low degree of oxidation of the chromium present in the waste.

There is a significant participation of water-soluble compounds in the particulate matter.

The low concentration of CO in the flue gas indicates a high combustion efficiency for the process.

A significant reduction of the NO emissions, compared to the results obtained in the combustion of footwear leather waste in fluidized bed, was observed.

The footwear leather waste (biomass) represents an alternate source for the generation of energy.

ACKNOWLEDGEMENTS

To Preservar-Tratamento e Reciclagem de Resíduos and Luftech-Soluções Ambientais for technical and financial support, to CAPES, CNPq and FINEP for financial support.

REFERENCES

- Minchener, A. J.; Coal gasification for advanced power generation. *Fuel* **84**, 2222-2235, 2005.
- Malkow, T.; Novel and innovative pyrolysis and gasification technologies for energy efficient and environmentally sound MSW disposal. *Waste Management* **25**, 53-79, 2004.
- Henriksen, U.; Ahrenfeldt, J.; Jensen, T. K.; Gøbel, B.; Bentzen, J. D.; Hindsgaul, C.; Sørensen, L. H.; The design, construction and operation of a 75 kW two-stage gasifier. *Energy* **4**, 1542-1553, 2006.

- Aznar, M. P.; Caballero, M. A.; Sancho, J. A.; Francés, E.; Plastic waste elimination by co-gasification with coal and biomass in fluidized bed with air in pilot plant. *Fuel Processing Technology* **87**, 409-420, 2006.
- Stahl, K.; Waldheim, L.; Morris, M.; Jonhsson, U.; Gardmark, L.; Biomas IGCC at Värnamo, Sweden-Past and Future. *GCEP Energy Workshop*, 2004.
- Bowden, W.; Gasification-Achieving Zero Waste. *JALCA* **98**, 19-25, 2003.
- Belgiorno, V.; Feo, G. D.; Rocca, C. D.; Napoli, R. M.; A. Energy from gasification of solid wastes. *Waste Management* **23**, 1-15, 2003.
- Reed, T. B.; Das, A.; Handbook of Biomass Downdraft Gasifier Engine Systems; The Biomass Energy Foundation Press, second edition, 1988.
- Babu, B. V.; Sheth, P. N. Modeling and simulation of downdraft biomass gasifier. *Biochemical Engineering, ChemCon '04*, Mumbai, 2004.
- Zainal, Z. A.; Ali, R.; Lean, C. H.; Seetharamu, K. N. Prediction of performance of a downdraft gasifier using equilibrium modeling for different biomass materials. *Energy Conversion and Management* **98**, 1499-1515, 2001.
- Gómez-Moreno, F. J.; Sanz-Rivera, D.; Martín-Espigares, M.; Papameletiou, D.; Santi, G. D.; Kasper, G. Characterization of particulate emissions during pyrolysis and incineration of refuse derived fuel. *Journal of Aerosol Science* **34**, 1267-1275, 2003.
- Taborski, W.; Kowalski, Z.; Wzorek, Z.; Konopka, M. Thermal utilization of leather scrap after chrome tanning. *JALCA* **100**, 344-353, 2005.
- Duo, W.; Leclerc, D. Thermodynamic and kinetic studies of dioxin formation and emissions from power boilers burning salt-laden wood waste. *Organohalogen Compounds* **66**, 1008-1017, 2004.
- Griffin, R. D.; A new theory of dioxin formation in municipal solid waste combustion; *Chemosphere* **15**, 1987-1990, 1986.
- Environmental Protection Agency (EPA); Guidance on Setting Permit Conditions and reporting Trial Burn Results, 1989.
- Kanuri, A. M.; Introduction to Combustion Phenomena; Gordon and Breach Science Publishers, 1975.
- Leppälähti, J.; Koljonen, T.; Nitrogen evolution from coal, peat and wood during gasification: Literature review. *Fuel Processing Technology* **43**, 1-45, 1995.
- Schäfer, S.; Bonn, B.; Hydrolysis of HCN as an important step in nitrogen oxide formation in fluidized combustion. Part 1. Homogeneous reactions; *Fuel* **79**, 1239-1246, 2000.
- Berger, A.; Rotzoll, G.; Kinetics of NO reduction by CO on quartz glass surfaces; *Fuel* **74**, 452-455, 1995.
- Bahillo, A.; Armesto, L.; Cabanillas, A.; Otero, J.; Thermal valorization of footwear leather wastes in bubbling fluidized bed combustion; *Waste Management* **24**, 935-944, 2004.

NOTATION

A:	cross-section area (m^2)	P:	product
C_p :	specific heat capacity (J/mol.K)	R:	reagent
F:	flow rate	T_1 :	ambient temperature (K);
H_f :	heat of formation (J/mol)	T_2 :	reduction zone temperature (K)
H_{vap} :	heat of vaporization (J/mol)	\bar{T} :	zone temperature (K)
HHV:	higher heating value (kcal/kg)	VS:	venturi scrubber
JVS:	jet venturi scrubber	V:	zone volume (m^3)
K:	equilibrium constant	v:	fluid velocity (m/s)
L:	characteristic dimension (m)	w:	mol H_2O per mol waste
LHV:	lower heating value (kcal/kg)	x:	n^o mols per mol waste
m:	mol O_2 per mol waste	y:	mole fraction
m' :	volume of gas generated per kg of leather fed (Nm^3/kg)	ρ :	fluid density (kg/m^3)
m_{air} :	air flow rate (kg/h)	μ :	fluid viscosity (kg/s.m)
P:	pressure (atm)	ϕ_p :	particle diameter (μm)
		Δh :	enthalpy change (J/mol)
		ΔH_c :	heat of combustion (J/mol)